



1 Review

2 **O⁶-alkylguanine-DNA alkyltransferases in microbes** 3 **living on the edge: from stability to applicability**

4 **Rosanna Mattossovich[§], Rosa Merlo[§], Riccardo Miggiano[‡], Anna Valenti^{^*} and Giuseppe**
5 **Perugino^{^*}**

6 [^]Institute of Bioscience and BioResources, National Research Council of Italy, Via Pietro Castellino 111, 80131
7 Naples, Italy; rosanna.mattossovich@ibbr.cnr.it, rosa.merlo@ibbr.cnr.it

8 [‡]Department of Pharmaceutical Sciences, University of Piemonte Orientale, Via Bovio 6, 28100 Novara, Italy;

9 riccardo.miggiano@uniupo.it

10 * Correspondence: anna.valenti@ibbr.cnr.it; Tel.: +39-081-6132-247 (A.V.)

11 * Correspondence: giuseppe.perugino@ibbr.cnr.it; Tel.: +39-081-6132-496 (G.P.); Fax: +39-081-6132-646

12 Received: date; Accepted: date; Published: date

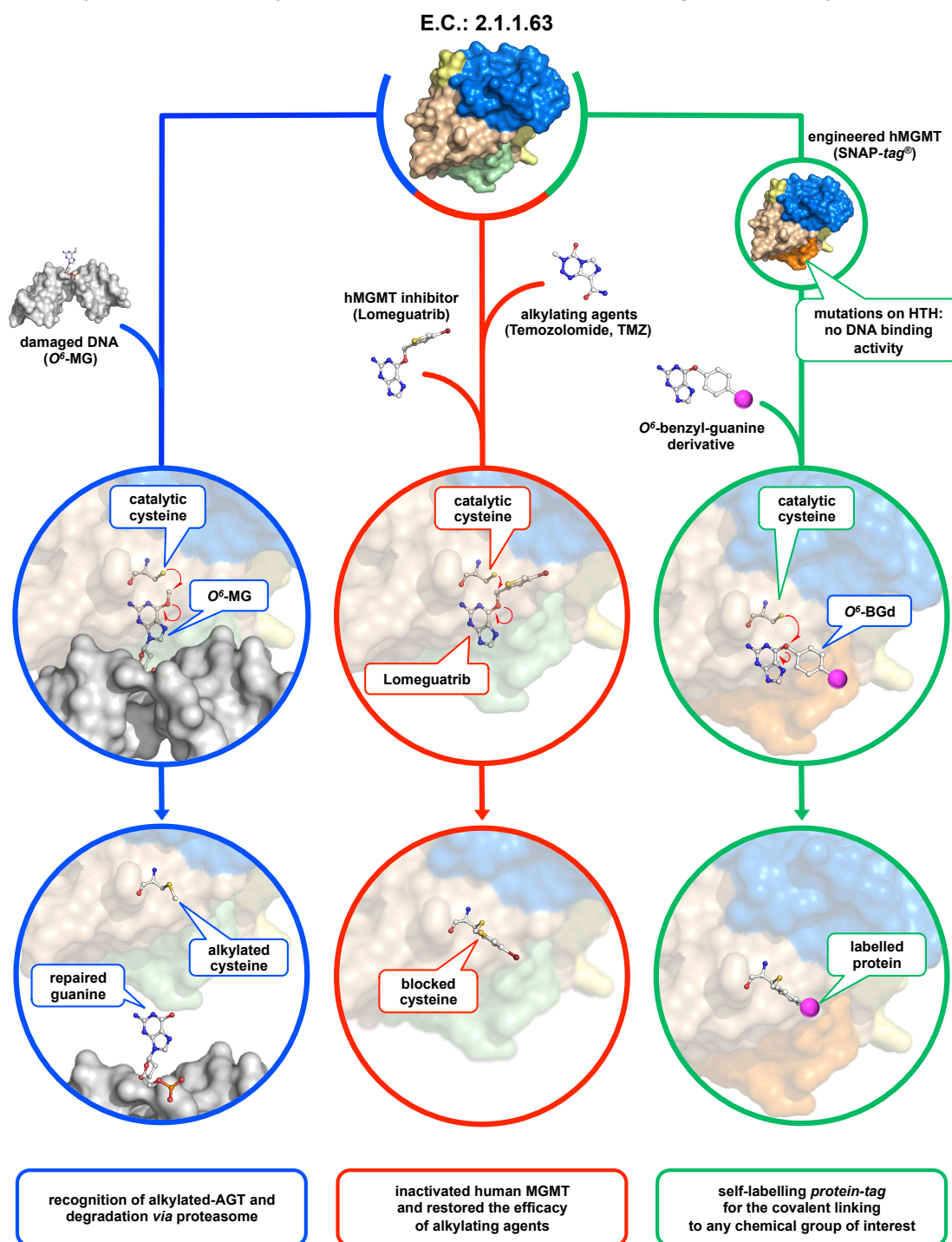
13 **Abstract:** The genome of living cells is continuously exposed to endogenous and exogenous
14 attacks, and this is particularly amplified at high temperatures. Alkylating agents cause DNA
15 damage leading to mutations and cell death; for this reason, they also play a central role in
16 chemotherapy treatments. A class of enzymes, defined AGTs, are evolutionarily suitable for the
17 DNA protection caused by alkylating agents, in particular in the recognition and repair of
18 alkylated guanines in O⁶-position. The peculiar irreversible trans-alkylation reaction of these
19 enzymes has triggered numerous studies, especially on the human homologue, as from the point
20 of view of basic research, in order to identify effective inhibitors in the fight against cancer, as well
21 as in the modern biotechnology, with the preparation of engineered variants to be used as
22 *protein-tags*. In the last decade, efforts have been made in the characterization of AGTs from
23 (hyper)thermophilic sources as useful model systems that have allowed the clarification of
24 numerous phenomena, common also to mesophilic enzymes. This review traces recent progresses
25 on this class of *thermozymes*, emphasizing their usefulness in basic research and the consequent
26 advantages in *in vivo* and *in vitro* biotechnological applications under non-permissive reaction
27 conditions.

28 **Keywords:** thermophilic sources; DNA repair; biotechnological tools, alkylation damage; AGT

29 1. Introduction

30 Monofunctional alkylating agents, a class of mutagenic and carcinogenic agents present in the
31 environment, induce DNA alkylation in several positions, as guanine at O⁶ (O⁶-MG; 6 % of adducts
32 formed), 7-methyl-guanine (N⁷-MG; 70 %), and 3-methyl-adenine (N³-MA; 9 %) [1]. Among them,
33 O⁶-alkylation of guanines (O⁶-AG) is a cytotoxic lesion: although the specific mechanism of this
34 cytotoxicity is not explicated, it was proposed that the toxic effect occurs after DNA replication,
35 because the O⁶-AG incorrectly matches with thymine generating a transition from G:C to A:T [2].
36 The O⁶-MG elimination abnormalities that occur at the time of replication are recognized by the
37 post replication mismatch repair system with potential harmful implications for cell viability. Apart
38 from conventional DNA repair multi-step pathways (as MMR, NER, BER, etc.), alkylated-DNA
39 protein alkyl-transferases (called AGT, OGT, or MGMT; EC: 2.1.1.63) perform the direct repair of
40 alkylation damage in DNA [3, 4]. They represent the major factor in counteracting the effects of
41 alkylating agents that form such adducts [4]. These are small enzymes (17-22 kDa) and widely
42 present in organisms of the three living kingdoms (bacteria, archaea, eukaryotes) but apparently
43 absent from plants, *Schizosaccharomyces pombe*, *Thermus thermophilus* and *Deinococcus radiodurans*.
44 The reaction mechanism of AGTs is based on the recognition of the damaged nucleobase on DNA

45 [5], followed by a one-step SN₂-like mechanism, in which the alkyl group of the damaged guanine
 46 is irreversibly transferred to a cysteine residue in its active site [5-8] (Figure 1, *blue way*).



47

48 **Figure 1.** *The AGTs' world.* The peculiar irreversible reaction mechanism of these enzymes plays a pivotal
 49 role in the physiological DNA repair (*blue way*), and it has important repercussions in the cancer cells
 50 treatment (*red way*) and biotechnological applications (*green way*). Atoms are colored by the CPK
 51 convention.

52 For these reasons, they are also called *suicide* or *kamikaze* proteins, showing a 1:1 stoichiometry of
 53 their reaction with the natural substrate. The disadvantage of this elegant catalysis is that, upon
 54 alkylation, the protein is self-inactivated and destabilized, triggering its recognition by cellular
 55 systems to be addressed to the proteasome [8, 9].

56

57 1.1 AGTs as target in cancer therapy

58 Alkylation damage to DNA occurs in various living conditions, and for this reason the
59 widespread presence of AGT protects cells from killing by means of alkylating agents. However,
60 human AGT (hMGMT) is a *double-edged* sword: on the one hand, it protects healthy cells from these
61 genotoxic and carcinogenic effects; on the other hand, it counteracts alkylating agents-based
62 chemotherapy by also protecting cancer cells from the killing effect of these drugs [10, 11].
63 Consequently, hMGMT has emerged as a crucial factor in anticancer therapies [12]: in recent years,
64 in fact, an inverse relationship has been discovered between the presence of hMGMT and the
65 sensitivity of cells to the cytotoxic effects of alkylating agents, such as temozolomide (TMZ), in
66 different types of cancer cells, including prostate, breast, colon and lung cancer cells [13].

67 The resistance to chemotherapy may be reduced by inhibition of these enzymes: as described
68 before, after removing the lesion, the alkylated form of the protein is inactivated and irreversibly
69 addressed towards intracellular degradation pathways. Hence, in order to counteract the action of
70 hMGMT under chemotherapy regimens, a large number of studies have been aimed to the
71 development of hMGMT inactivators to be used in combination with alkylating agents. In view of
72 this therapeutic relevance, much success has been obtained through the design of hMGMT
73 pseudo-substrates, namely the *O*⁶-benzylguanine (*O*⁶-BG) and the strong inactivator
74 *O*⁶-[4-bromophenyl]-guanine (*O*⁶-BTG, Lomeguatrib) [13, 14]. These compounds mimic damaged
75 guanine on DNA and reacts with the protein by the covalent transfer of the alkyl adduct to the
76 active site cysteine residue, causing the irreversible inactivation of the enzyme (Figure 1, *red way*).
77 Therapeutically, *O*⁶-BG is not toxic on its own, but makes cancer cells 2 to 14 times more sensitive to
78 alkylating agents' effects. The oligonucleotides containing more *O*⁶-BG are potent inhibitors and
79 represent a valid alternative to the use of free modified guanines to improve the activity of the
80 alkylating chemotherapy drug in the treatment of some classes of tumors [15, 16, 17].

81 1.2 AGTs and biotechnology

82 The specific labelling of proteins with synthetic probes is an important advance for the study
83 of protein function. To achieve this, a way is through the expression of the protein of interest in
84 fusion with additional genetically encoded polypeptides, called *tags*, which mediates the labelling.
85 The first great example of an *autofluorescent tag* was the *Aequorea victoria* green fluorescent protein
86 (GFP) allowing the *in vivo* localization of fusion proteins in cellular and molecular biology fields
87 [18, 19]. Among *affinity tags*, of particular importance are the poly(His)-*tag*, the chitin-binding
88 protein, the maltose binding protein [20], the Strep-*tag* [21] and the glutathione-S-transferase
89 (GST-*tag*) [22], which allow fast and specific purification of proteins of interest from their crude
90 biological source using affinity techniques. *Solubilization tags* are especially used to assist the proper
91 folding of recombinant proteins expressed in chaperone-deficient species such as *Escherichia coli*,
92 avoiding protein precipitation: these include the thioredoxin [23] and the poly(NANP).

93 However, all the *tags* listed above are limited by the fact that each of them can be used for one
94 or some fields of application. The need therefore emerged to somehow use a *universal tag* that could
95 widely cover modern biotechnology.

96 To overcome these issues, in 2003 the group headed by Kai Johnsson pioneered the use of an
97 engineered hMGMT variant as fusion protein for *in vitro* and *in vivo* biotechnology applications,
98 which led then to its commercialization, namely SNAP-*tag*[®] (New England Biolabs) [24-27]. They
99 started from the knowledge that hMGMT tolerates very well the presence of groups conjugated to
100 the pseudo-substrate *O*⁶-BG (*O*⁶-BG derivatives): the unusual covalent bond with the benzyl moiety
101 can therefore be exploited for "biotech" purposes (Figure 1, *green way*). Thanks to its small size,
102 SNAP-*tag*[®] can be fused with other proteins of interest: the expression of the fusion protein inside
103 the cells followed by incubation with opportune fluorescent derivatives leads to *in vivo* labelling
104 and localization of fusion proteins with the probe [24]. The same principle has also been used for
105 the *in vitro* immobilization of tagged fusion proteins: in this case, the *O*⁶-BG is attached to a surface
106 at an adequate distance in order to prevent the enzymatic reaction [28]. This offers a delicate

107 condition for fixing and disposing in a better orientation a wide range of proteins/enzymes on a
 108 surface. The SNAP-tag® technology was successfully applied to Surface Plasmon Resonance (SPR)
 109 for the covalent immobilization of proteins of interest [29]. Another interesting application of this
 110 protein-tag is the possibility to produce new antibody fragments (scFv-SNAP) to be employed in
 111 the SPR analysis [30].

112 Despite the need to use a specific substrate, SNAP-tag® offers endless applications: the
 113 possibility to covalently link a desired chemical group (conjugated to the O⁶-BG) to a protein of
 114 interest (genetically fused to it), makes it decidedly advantageous, if compared to traditional
 115 *protein-tags* currently in use. Table 1 shows a brief comparison between some examples of
 116 *protein-tags* and the SNAP-tag® in several application fields.

117 **Table 1.** The use of *protein-tags* in some applicative examples.

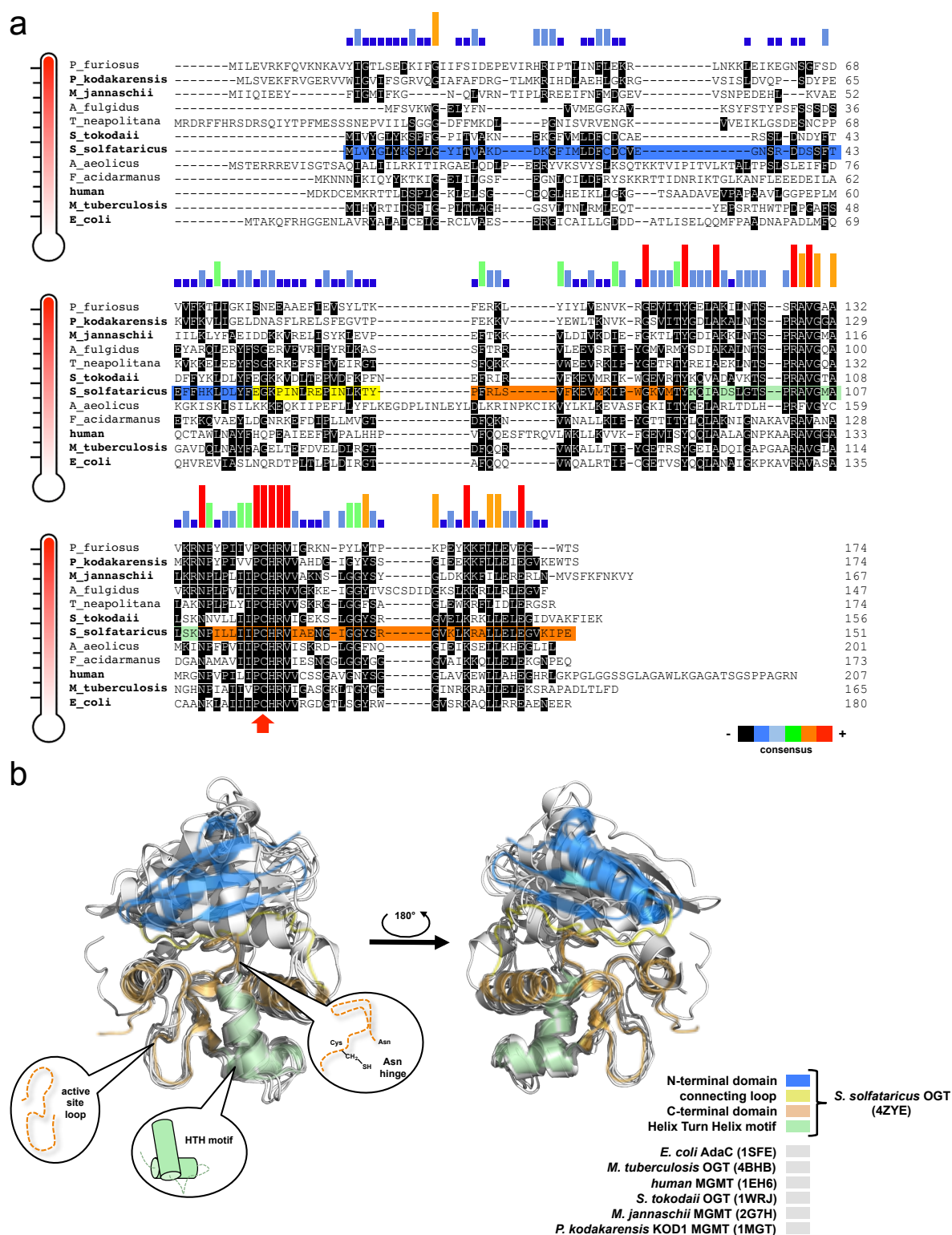
Applications.	FPs	affinity tag	SNAP-tag®	notes
<i>in vivo</i> imaging	+ ^a	-	+	
substrate utilization	+	-	-	FPs do not need of any substrate for their fluorescence
emission spectra	±	-	+	FPs are in a limited number respect to chemical probes
time-resolved fluorescence	±	-	+	
multi-color fluorescence	±	-	+	for FPs, multi-cloning and expression is necessary
<i>in vitro</i> applications	±	±	+	
variety of chemical group labelling	-	-	+	
pulse-chase analysis	-	-	+	fresh synthesized FPs cannot be efficiently quenched
anaerobic conditions	-	+	+	FPs' fluorophore formation requires oxygen
protein purification	-	+	+	
protein immobilization	±	+	+	immobilized anti-FPs antibody required
pull-down experiments	±	+	+	anti-FPs antibody required

118 ^a+, fully applicable or advantageous; ±, limited applicability; -, not applicable or disadvantageous.

119 2. Thermophilic and thermostable AGTs

120 As for organisms living under mesophilic conditions, environmental and endogenous
 121 alkylating agents also attack thermophilic and hyper-thermophilic organisms' genomes.
 122 Additionally, high temperatures accelerate the process of formation of alkylated bases, leading to
 123 DNA breaks [31]. These agents are chemically unstable at the physiological conditions of these
 124 organisms, however the collateral decomposition may worsen the formation of DNA alkylation
 125 products [32]. Thus, the presence of AGTs and methylpurine glycosylases in hyperthermophilic
 126 organisms implies they are naturally exposed to endogenous methylating agents [32], supporting
 127 the crucial role of AGTs, even if limited information is available on these thermostable proteins [33,
 128 34].

129 Apart from some studies on Archaea using cell free extracts, few examples of biochemical
 130 characterization of AGT from thermophilic sources is that of the enzymes from *Pyrococcus* sp. KOD1
 131 [33] conducted by Imanaka and co-workers, and from *Aquifex aeolicus* and *Archaeoglobus fulgidus*
 132 performed by the group of Prof. Pegg in 2003 (Figure 2) [32]. In particular, *A. aeolicus* AGT, whose
 133



135

136

137

138

139

140

141

Figure 2. (a) Alignment of biochemically and structurally (*in bold*) characterized AGTs. DNA sequences are listed in decreasing order of temperature. The histograms in different colours show the sequence consensus, and the red arrow indicates the highly conserved catalytic cysteine. (b) Superimposition of all known AGT structures in their free form (*in grey*). All common domains and elements are coloured only for the SsOGT enzyme. Coloured bars behind the SsOGT sequence in (a) recall the enzyme domains highlighted in the structure and in the legend in (b).

142 organism was identified as the most primitive bacterium, is closer to the mammalian AGTs than
143 other bacterial homologues in terms of O⁶-BG sensitivity [32].

144 2.1 The common themes in AGTs' tertiary structure and the intrinsic factors of stability

145 Despite the different primary structures (Figure 2a), thermophilic enzymes showed a typical
146 AGT protein architecture, consisting of two domains [35]: a highly conserved C-terminal domain
147 (C_{ter}), surprisingly superimposable for all the AGT structures available on common protein data
148 banks (Figure 2b), and a N-terminal domain (N_{ter}), which is very different among AGTs and whose
149 function is not well fully addressed (likely involved in regulation, cooperative binding and stability
150 [6, 38, 39]). The C_{ter} contains the DNA binding helix-turn-helix motif (HTH), the *Asn hinge*, which
151 precedes the -V/IPCHRVV/I- amino acid sequence of the active site (except the *Caenorhabditis*
152 *elegans* AGT-2 that has the -PCHP- sequence [36, 37]), and the *active site loop*, responsible for the
153 substrate specificity.

154 Apart from external factors that could contribute in protein stability, such as the binding to
155 substrate or cofactor [40], to selective ligands [41] and to partner protein [42], the stability and the
156 functional folding of a biological macromolecule is often related to intrinsic factors. A comparative
157 structural analysis performed on AGT proteins whose structures have been deposited in the Protein
158 Data Bank reveals significant differences on the intrinsic structural features that have been
159 considered relevant for thermostability, such as helix capping, intramolecular contacts (hydrogen
160 bonds, ion-pairs), and solvent accessible surface areas. Helix capping plays a central role in the
161 stability of α -helices, due to lack of *intra*-helical hydrogen bonds in the first and last turn [43, 44],
162 and its effect results in an overall structural stabilization of protein folding [45]. By inspecting the
163 crystal structure of the OGT protein from the archaeon *Saccharolobus solfataricus* (hereinafter *SsOGT*)
164 (PDB ID: 4ZYE), considered here as the thermophilic reference, we verified that the five α -helices
165 composing the protein tertiary structure are characterized by the presence of helix capping,
166 possibly increasing the thermal stability. In particular, the helix *H1* at the N_{ter} is stabilised by a
167 peculiar double serine sequence (S40-S41) and a glutamic acid (E54) at its C_{ter}, the latter is strictly
168 conserved in all AGTs from thermophilic organisms (see Figure 2a). The helix-turn-helix motif
169 (HTH), built on helices *H3* and *H4*, is stabilized at level of *H3* by a highly conserved threonine
170 residue (T89) as N_{ter} capping and a serine (S96), distinctive of *SsOGT*, as C_{ter} capping. Furthermore,
171 helix *H4* contains two serine-based capping among which the one placed at N_{ter} (S100) is strictly
172 conserved in all thermophilic AGTs and is followed by a proline (P101) that fits well in the first turn
173 of the helix thanks to its own backbone conformation. Finally, the helix *H5* is protected by glutamic
174 acid capping that is present in all the AGTs from different species. Another feature contributing to
175 thermal stability is the solvent-accessible surface area (SASA); indeed, the decrease of SASA and the
176 increase of hydrophobic residues that are buried from the solvent atoms have been considered as
177 stabilized principles for thermostable protein [46]. As described in Table 2, *SsOGT* shows the
178 smaller total SASA value in line with its exceptional stability, on the contrary OGT from *M.*
179 *tuberculosis* [38, 47] has the higher value due to the peculiar conformation of both the active site loop
180 and the C-terminal tail that are exposed to the bulk solvent.

181 Finally, by comparing hyperthermophilic AGTs with the orthologs from mesophilic
182 organisms, in terms of atomic contacts between charged residues as well as intramolecular
183 hydrogen bonds (Table 2), significant differences emerged in the number of charged residues
184 contacts. As expected for thermostable proteins [48], *SsOGT*, as well as the proteins from *S. tokodaii*
185 and *P. kodakaraensis*, shows a larger number of electrostatic contacts, characterized by higher
186 bond-dissociation energy, with respect to hydrogen bonds for which we did not detect significant
187 differences among the analysed structures, apart from MGMT of *P. kodakaraensis* (*Pk*-MGMT).

188 Although the number of H-bonds is approximately similar across the AGTs from different
189 organisms, there should be differences in the position-related role of such bonds supporting overall
190 stability of thermophilic variants. With reference to *Pk*-MGMT, Hashimoto and co-workers detected
191 the same number of ion-pairs between the extremophilic protein and *E.coli* AdaC [50]; however,
192 more *intra* and *inter*-helix ion-pairs were found in *Pk*-MGMT. It was suggested an absence of

193 correlation between ion-pairs' position and stabilization in AdaC, whereas in *Pk*-MGMT the
 194 *intra*-helix ion-pairs act on secondary structure elements stabilizing the helices conformations and
 195 the *inter*-helix ion-pairs consolidate the inter-domain interactions enhancing the stability of the
 196 tertiary structure packing.

197 **Table 2.** Comparison of solvent-accessible surface area and intramolecule contacts.

T_{opt}	Organism (PDB ID)	Total SASA (Å ²)	charged residues contacts	intramolec ule H-bonds ^a	Refs
37 °C	<i>Escherichia coli</i> (1SFE)	8421.8	74	141	[50]
37 °C	<i>Mycobacterium tuberculosis</i> (4BHB)	9535.2	56	143	[38]
37 °C	<i>Homo sapiens</i> (1EH6)	8764.3	71	127	[6]
80 °C	<i>Saccharolobus solfataricus</i> (4ZYE)	8054.1	94	137	[39]
80 °C	<i>Sulfurisphaera tokodaii</i> (1WRJ)	8049.5	124	134	PDB ^b
80 °C	<i>Methanocaldococcus jannashii</i> (2G7H)	17770.8 ^c	N.D	N.D.	[51]
85 °C	<i>Pyrococcus kodakaraensis</i> KOD1 (1MGT)	8302.8	111	157	[49]

198 ^aExcluding intra-residues H-bonds. ^b<https://www.rcsb.org/structure/1wrj>. ^cThe structure has been solved by
 199 means of NMR explaining the high SASA value.

200 3. The O⁶-Alkylguanine-DNA-alkyltransferase from *Saccharolobus solfataricus*

201 In the last decade SsOGT has been identified and characterized through detailed physiological,
 202 biochemical and structural analysis. Due to its intrinsic stability, SsOGT protein has proven to be an
 203 outstanding model for clarifying the relationships between function and structural characteristics.

204 *S. solfataricus* (previously known as *Sulfolobus solfataricus*) is a microorganism first isolated and
 205 discovered in 1980 in the Solfatara volcano (Pisciarelli-Naples, Italy), which thrives in volcanic hot
 206 springs at 80 °C and a pH 2.0-4.0 range. In order to protect its genome in these harsh conditions, *S.*
 207 *solfataricus* evolved several efficient protection and repair systems [31, 52]. *S. solfataricus* is highly
 208 sensitive to alkylating agent methyl methane sulfonate (MMS), showing a transient growth arrest
 209 when treated with MMS concentrations >0.25 mM to 0.7 mM. [31, 52]. Interestingly, while the *ogt*
 210 RNA level increased after treatment, the relative enzyme concentration decreases, suggesting its
 211 degradation in cells in response to MMS and, in general, to a cellular stresses [52]. Under these
 212 treatment conditions, however, the protein level rises after few hours from the treatment, and, in
 213 parallel, the growth of *Saccharolobus* starts again [52], indicating a role of *ogt* in efficient DNA repair
 214 by alkylation damage.

215 3.1 Innovative OGT assays

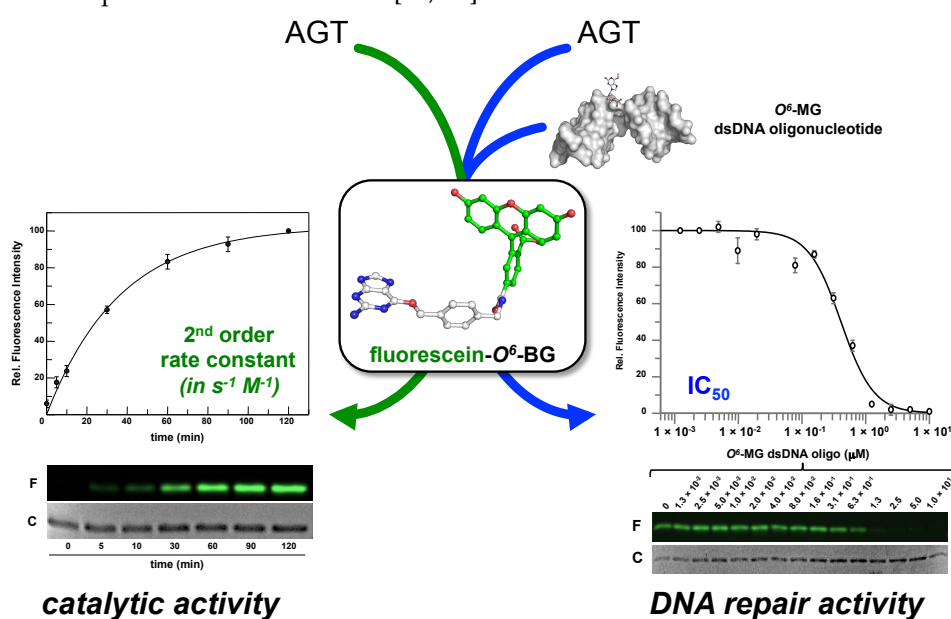
216 The attention of researchers, mainly on hMGMT, not only concerns the deepening of critical
 217 biological processes, such as DNA repair, but also the development of new and simple intuitive and
 218 economic assays, mainly aimed to optimize the inhibitory molecules of therapeutic interest in the
 219 cancer treatment. Various assays to measure AGT activity are reported in the literature. The first
 220 methods elaborated were based on the use of oligonucleotides carrying radioactive (³H or ¹⁴C)
 221 O⁶-alkylguanine groups. Proteinase K digestion was then carried out and to measure the levels of

222 marked S-methyl-cysteine in the lysate after an automatic amino acid analyser [53]. A very similar,
 223 but simpler and faster radioactive assay has been used: in this procedure, a ^{32}P terminal labelled
 224 oligonucleotide contains a modified guanine into a methylation-sensitive restriction enzyme
 225 sequence (as *Mbo* I). The AGT DNA repair activity leads to an unmethylated DNA, then target for
 226 the restriction enzyme [54]. This procedure was also used by the Ciaramella's group to identify for
 227 the first time the activity of SsOGT: this test had the advantage of analysing the fragment digested
 228 directly by electrophoresis on polyacrylamide gel [52].

229 It was therefore improved in terms of precision by the subsequent separation of the
 230 oligonucleotides digested by HPLC; however it resulted less simple to perform. The
 231 chromatographic separation allowed the calculation of the concentration of active AGT after
 232 measuring the radioactivity of the peak corresponding to the digested fragment [55]. Similarly,
 233 Luu's group developed the analysis of hMGMT reaction products in 2002, based on HPLC
 234 separation. This test investigated the degree of inhibition of oligonucleotides with O^6 -MG or O^6 -BG
 235 in different positions that varied from 3' to 5' end and whether they could be used as chemotherapy
 236 agents. IC_{50} values were obtained by quantifying the remaining active protein after the radioactive
 237 DNA reaction [56].

238 Although these assays allowed reliable, precise and direct measurements of protein activity,
 239 the use of radioactive materials and chromatographic separations make these assays long, tedious
 240 and unsafe. An alternative approach was proposed in 2010 by the group of Carme Fàbrega, who set
 241 up an assay based on the thrombin DNA aptamer containing a fluorophore and a quencher: the
 242 quadruplex structure of this oligonucleotide is compromised if a central O^6 -MG is present,
 243 hampering the two probes to stay closer. An AGT's repair activity on the oligonucleotide allows the
 244 folding of the quadruplex structure and the FRET taking place, resulting in a decrease of the
 245 fluorescence intensity [57].

246 Recently, the introduction of fluorescent derivatives of the O^6 -BG (as SNAP Vista Green®, New
 247 England Biolabs) makes possible the development of an innovative DNA alkyl-transferase assay.
 248 Thus, since AGT covalently bind a benzyl-fluorescein moiety of its substrate after reaction, it is
 249 possible to immediately load on a SDS-PAGE: the *gel-imaging* analysis of the fluorescence intensity
 250 gives a direct measure of the protein activity, since the 1:1 stoichiometry of protein/substrate
 251 (Figure 3). Signals of fluorescent protein (corrected by the amount of loaded protein by coomassie
 252 staining analysis) obtained at different times are plotted and a second order reaction rate is
 253 determined [38, 39, 47, 52, 58, 59]. This method can be applied to all those AGTs sensitive to O^6 -BG,
 254 with the exception of the *E. coli* AdaC [60, 61].



255
 256
 257

Figure 3. Innovative fluorescent AGT assay. The substrate could be used alone for the determination of the AGT catalytic activity, or in combination with a competitive non-fluorescent substrate

258 (alkylated-DNA). In the latter case an indirect measure of the DNA repair activity on natural
259 substrates is determined (adapted from [62]).

260 Furthermore, an alkylated dsDNA oligonucleotide can be included in a competition assays
261 with the fluorescein substrate. This non-fluorescent substrate makes lower the final fluorescent
262 signal on *gel-imaging* analysis, depending on its concentration. In this way, it is possible to measure
263 the activity of AGTs for their natural substrate, giving an indirect measure of methylation repair
264 efficiency (Figure 3) [38, 39, 47, 52, 58, 59]. By using this methodology, it was even possible to
265 discriminate the SsOGT activity regarding the position of the O⁶-MG on DNA (see below; [39]), in
266 line with previous data on hMGMT [63].

267 3.2 Biochemical properties of *S. solfataricus* OGT

268 The recombinant SsOGT protein, heterologously expressed in *E. coli*, has been fully
269 characterized using the fluorescent assay described in paragraph 3.1 and showed in Table 3. In
270 agreement with its nature, the protein showed optimal catalytic activity at 80 °C, although retaining
271 a residual activity at lower temperatures (Table 2), and in a pH range between 5.0 and 8.0. As for
272 the most part of thermophilic enzymes, SsOGT is resistant over a wide range of reaction conditions,
273 such as ionic strength, organic solvents, common denaturing agents and proteases [52, 58].
274 Interestingly, chelating agents do not affect the activity of this enzyme: crystallographic data
275 clarified that the archaeal enzyme lacks a zinc ion in the structure [39], whereas this ion is important
276 for the hMGMT correct folding [6].

277 3.3 Crystal structure of SsOGT

278 All the steps of the AGTs' activity (alkylated DNA recognition, DNA repair, irreversible
279 trans-alkylation of the catalytic cysteine, recognition and degradation of the alkylated protein) have
280 been structurally characterized. Most knowledge these proteins come from classic studies on
281 hMGMT, as well as the Ada-C and OGT from *Escherichia coli* [5-8, 50], but other AGTs' structures
282 are also available in the Protein Data Bank site (Figure 2a) ([http://www.rcsb.org/
283 pdb/results/results.do?tabtoshow=Current&qrid=D3B02F3B](http://www.rcsb.org/pdb/results/results.do?tabtoshow=Current&qrid=D3B02F3B)).

284 As described in Figure 1, all AGTs are inactivated after the reaction and degraded *via*
285 proteasome, but in higher organisms, the degradation is preceded by protein ubiquitination [9]. It is
286 common opinion that the recognition of alkylated-AGTs is due by a conformational change:
287 however, data on structure and properties of alkylated AGTs are limited because alkylation greatly
288 destabilizes their folding [39]. The methylated-hMGMT and benzylated-hMGMT 3D structures
289 were only obtained by flash-frozen crystals, showing that alkylation on the catalytic cysteine (C145)
290 induces subtle conformational changes [6, 7, 64]; consequently, these structures might not reflect the

291 **Table 3.** Biochemical properties comparison among SNAP-tag[®], SsOGT wt and the relative H⁵
292 mutant.

	SNAP-tag [®]	SsOGT	SsOGT-H ⁵
molecular weight (kDa) ^a	23.0	17.0	17.0
T _{opt} (°C)	37.0	80.0	75.0
relative activity			
at 25.0 °C	80 %	25 %	50 % ^b
at 37.0 °C	100 %	45 %	65 %
at 80 °C	-	100 %	95 %
catalytic activity at 37 °C	2.8 × 10 ⁴	2.8 × 10 ³	1.6 × 10 ⁴
pH _{opt}	6.0	7.5	6.0
thermal stability T _{1/2} (°C)	6 h (37)	3 h (70)	3 h (70)
thermal stability T _{1/2} at 37 °C	6 h	> 24 h	> 24 h
additives			
NaCl	< 0.3 M	> 1.0 M	> 1.0 M
EDTA	no	yes	yes
sarcosyl	no	> 0.5 %	> 0.5 %

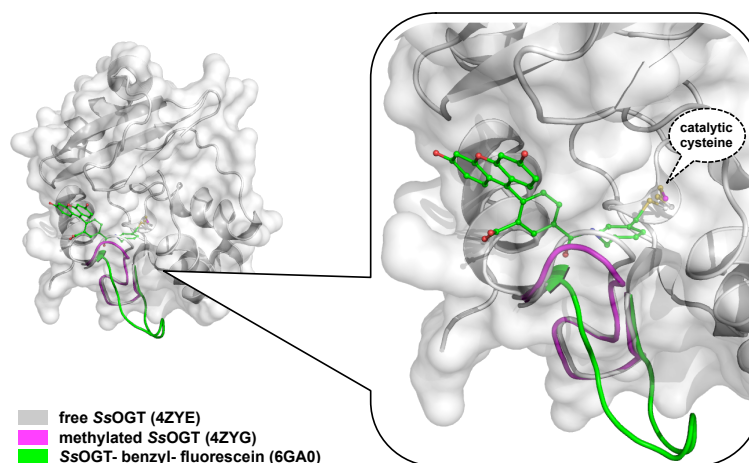
DDT	yes	no	no
	^a data from [52, 58, 65]. ^b enhancement respect to the SsOGT wt (<i>in bold</i>).		

293

294 physiological conformation of the alkylated hMGMT, since in the crystalline state the protein could
295 not accurately display the conformation adopted in solution [39].

296 Concerning the interactions with the DNA, SsOGT binds methylated oligonucleotides: the
297 repair activity depends on the position of the alkyl-group [39]: to efficiently repair the alkylated
298 base on dsDNA, the protein requires at least 3 bases from either the 5' or the 3' end. This is due to
299 the necessary interactions formed with the double helix. Structural analysis confirmed these data
300 [39].

301 Considering that AGTs have a highly conserved C_{ter} domain, efforts were put on thermostable
302 homologues of the hMGMT. In contrast to the human counterpart, SsOGT was soluble and
303 relatively stable, thus allowing *in-deep* analysis of the protein in its post-reaction form [39].
304 Structural and biochemical analysis of the archaeal OGT, as well as after the reaction with a bulkier
305 adduct in the active site (benzyl-fluorescein; [66]), suggested a possible mechanism of
306 alkylation-induced SsOGT unfolding and degradation (Figure 4). Based on their data, Perugino and
307



308

309 **Figure 4.** Conformational changes of the SsOGT *active site loop* upon the methyl (*in magenta*) or the
310 benzyl-fluorescein (*in green*) irreversible transfer [39, 66].

311 co-workers suggested a general model for the mechanism of post-reaction AGTs destabilization: the
312 so called *active-site loop* moves towards the bulk solvent as result of the covalent binding of alkyl
313 adduct on the catalytic cysteine and *the extent of the loop movement and dynamic correlates with the*
314 *steric hindrance of the adduct* [39, 66] (Figure 4). The destabilization of this protein region triggers the
315 recognition of the alkylated protein to be addressed to degradation pathway.

316 3.4 Biotechnological applications of an engineered SsOGT, the H⁵ mutant

317 Apart from new examples of thermostable auto-fluorescent protein (FPs) variants have been
318 exploited in thermophilic microorganisms [67], the general use of most of *protein-tags* is limited only
319 to mesophiles and in mild reaction conditions. As described in paragraph 1.2, the introduction of
320 the SNAP-tag[®] technology enabled a wide *in vivo* and *in vitro* labelling variety for biological studies
321 by fusing any protein of interest (POI) to this *protein-tag* [68]. However, being originated from
322 hMGMT, the application to extremophilic organisms and/or to harsh reaction conditions is
323 seriously limited.

324 By following the same approach used for the hMGMT by Kai Johnsson, an engineered version
325 of SsOGT has been produced [52, 58]. This protein, called SsOGT-H⁵, presents five mutations in the
326 helix-turn-helix domain, abolishing any DNA binding activity [52]. In addition, a sixth mutation
327 was made: in the *active site loop*, where a residue of serine was replaced by a glutamic acid at
328 position 132 (S132E). This modification increased the catalytic activity of SsOGT [52, 58], as it was

329 observed in the engineered version of the hMGMT along the SNAP-tag® development [24]. H⁵
330 shows slightly lower heat stability in respect to the wild-type protein (Table 3), while the resistance
331 to other denaturing agents is maintained. Moreover, SsOGT-H⁵ is characterised by a surprisingly
332 increased catalytic activity at lower temperatures, keeping the rate of reaction to the physiological
333 ones (Table 3) [52, 58]. These behaviours made this mutant a potential alternative to SNAP-tag® for
334 *in vivo* and *in vitro* biotechnological applications. The stability against thermal denaturation allowed
335 Miggiano and co-workers to obtain the structure of the protein after the reaction with the
336 fluorescent substrate SNAP-Vista Green®, unrevealing the peculiar destabilization of the *active site*
337 *loop* upon reaction [66].

338 3.4.1 *In vitro* thermostable H⁵-based chimeras

339 The *Saccharolobus* OGT mutant has been firstly tested as *protein-tag* fused to two thermostable
340 *S. solfataricus* proteins and in *E. coli* heterologous expressed. The chimeric proteins were correctly
341 folded in *E. coli* cells, and the *tag* did not interfere with the enzymatic activity of the tetrameric
342 β-glycosidase [58], nor with the hyperthermophile-specific DNA topoisomerase reverse gyrase
343 [69-73]. Furthermore, the stability of H⁵ made possible a heat treatment of the cell-free extract to
344 remove most of the *E. coli* proteins, as well as the β-glycosidase assay performed at high
345 temperatures, without the need of removing the tag before [58].

346 3.4.2 Expression in thermophilic organisms models

347 The applicability of the thermostable *tag* under *in vivo* conditions is fundamental: for this
348 reason H⁵ was also expressed in thermophilic organisms, taking advantage of the availability of the
349 fluorescent AGT assay allowed to establish the presence of H⁵ both in living cells as well as *in vitro*
350 in cell-free extracts [58, 73]. To address the activity to H⁵, it was necessary to choose models in
351 which endogenous AGT activity is suppressed. *Thermus thermophilus* is a *ogt*⁽⁻⁾ species, showing only
352 an *agt* homologue (TTHA1564), whose annotation corresponds to an alkyltransferase-like protein
353 (ATL) [74]. ATLs are a class of proteins present in prokaryotes and lower eukaryotes [75],
354 presenting aminoacidic motifs similar to those of AGTs' C_{ter}, in which a tryptophan residue replaces
355 the cysteine in the active site [76]. Like AGTs, ATLs use a helix-turn-helix motif to bind the minor
356 groove of the DNA, but they do not repair it, aim to indeed to recruit and interact with proteins
357 involved in the Nucleotide Excision Repair system [77].

358 While *T. thermophilus* is a naturally *ogt* knockout organism, *Sulfolobus islandicus* possesses an
359 *ogt* gene very similar to that of *S. solfataricus* and it was silenced by a CRISPR-based technique and
360 was used as a host organism [73].

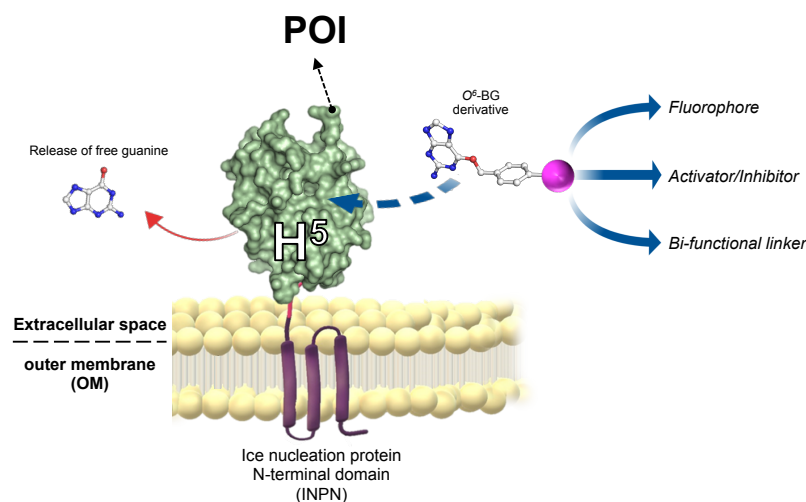
361 The fluorescent signal obtained by SDS-PAGE *gel-imaging* analysis revealed that SsOGT-H⁵ not
362 only is efficiently expressed in these thermophilic microorganisms, but it also shows that this *tag*
363 was correctly folded and active, demonstrating that H⁵ might be used as an *in vivo protein-tag* at
364 high temperatures [58, 73]. Moreover, the use of a fluorescent assay offers another opportunity: as
365 for the human cells, by using different fluorescent substrates, the pathways of POI fused to
366 SsOGT-H⁵ could be followed inside living “*thermo cells*”.

367 3.4.3 The ASL^{tag} system

368 As it is known, most of the biotechnological processes require harsh operational conditions. To
369 overcome the general instability of most of biocatalysts used in the processes, the introduction of
370 immobilised enzymes on solid supports has been helpful for their application [78]. By definition, an
371 immobilized enzyme is a “physically confined biocatalyst, which retains its catalytic activity and
372 can be used repeatedly” [79]. In fact, protein immobilisation offers several advantages, as the
373 catalysts recovery and reuse and the physical separation of the enzymes from the reaction mixture.
374 Currently, different immobilisation strategies are available, from physical adsorption to the
375 covalent coupling [80-83]. However, all these procedures require purified biocatalysts and arduous

376 techniques, as well as problems related to steric hindrance between the catalyst, the substrate and
 377 the solid support, with an increasing of costs and time for the production processes.

378 The introduction of “cell-based” immobilisation systems resulted in a significant improvement
 379 and reduce times and costs of the process. One of the most used display strategies is the
 380 simultaneous heterologous expression of enzymes and their *in vivo* immobilisation on the external
 381 surface of Gram-negative bacteria cells, by the utilisation of the ice nucleation protein (INP) from
 382 *Pseudomonas syringae* [84, 85]. Most recently, the N-terminal domain of INP (INPN) was used to
 383 produce a novel anchoring and self-labelling protein tag (hereinafter ASL^{tag}). The ASL^{tag} consists of two
 384 moieties, the INPN and the engineered and H⁵ mutant (Figure 5) [86].



385

386 **Figure 5.** The ASL^{tag} system. A protein of interest (POI) is genetically encoded with the *tag*, which in
 387 turn makes it anchored and exposed to the solvent, and contemporary able to covalently link to a
 388 desired chemical group (*magenta sphere*) by the activity of SsOGT-H⁵ (adapted from [87]).

389 The former allowed an *in vivo* immobilisation on *E. coli* outer membrane of enzymes of interest,
 390 making direct exposition of the enzyme to the solvent possible, leading to a significant reduction of
 391 the costs related to purification and immobilization, and to overcoming of problems related to the
 392 recovery of enzymes in a process [88]. The latter gives the unique opportunity to label the
 393 immobilized enzyme with any desired chemical groups (covalently link to the benzyl-guanine) [25,
 394 58], dramatically expanding biotechnological applications. In particular, it can be possible to
 395 modulate the activity of enzymes fused with the ASL^{tag} by introducing activators or inhibitors
 396 molecules or connecting them to other biocatalysts by using bi-functional linkers to improve
 397 cascade reactions (Figure 5). The ASL^{tag} system allowed the expression and immobilization of
 398 enzymes of interest, from monomeric proteins (e.g., the thermostable carbonic anhydrase from
 399 *Saccharolobus*, SspCA) to enzymes having a complex quaternary structure (e.g., the thermophilic
 400 SsβGly), without affecting their folding and catalytic activity [86]. Moreover, this system was also
 401 useful to stabilise fused proteins, as was the case for SspCA, which showed an increase in residual
 402 activity of up to 30% for a period of 10 days at 70 °C [87], representing a huge advantage in pushing
 403 beyond reactions in bioreactors and in the reutilization of biocatalysts.

404 4. *Pyrococcus furiosus* and *Thermotoga neapolitana* OGT

405 To date, no *protein-tags* have been applied at extremely high temperatures. Aimed to employ
 406 the SNAP-*tag*[®] technology to hyperthermophilic microorganisms for *in vivo* studies, it has been
 407 recently characterized an O⁶-alkylguanine-DNA alkyltransferase from the archaeon *Pyrococcus*
 408 *furiosus* [89]. This extremophilic microorganism was originally isolated from hot marine sediments
 409 in Vulcano Island (Italy) [90] with an optimum growth temperature around 100 °C and thriving
 410 under extremely harsh conditions. As other thermophilic Archaea, its enzymes are extremely

411 thermostable and find applicability in various biotechnological applications. Just think to one of the
412 most famous and used enzymes from *P. furiosus*: the DNA polymerase I, also known as *Pfu* DNA
413 polymerase, with a strong 3'-5' proof-reading activity [91]. The first demonstration of an OGT activity
414 in *P. furiosus* was in 1998, when Margison and co-workers identified a protein of 22 kDa, whose
415 catalytic activity was abolished by the O⁶-BG pseudo-substrate. The PF1878 ORF is relative to a
416 protein of 20.1 kDa: from the primary structure, the relative polypeptide seems to be relatively
417 closed to the MGMT from *Pyrococcus kodakarensis* KOD1 (*Pk*-MGMT) [49, 89, 92]. The extreme
418 thermostability was confirmed by *in vitro* biochemical studies on the heterologous expressed and
419 characterized *Pfu*OGT protein. This enzyme was active on BG-fluorescent substrates, allowing the
420 competitive assay with methylated dsDNA. However, the experiments were performed at 65 °C
421 instead of the standard procedure at 50 °C, as described for *Ss*OGT [39, 58, 59], due to a strong
422 thermophilicity of this enzyme. This behaviour was effectively confirmed by Differential Scan
423 Fluorimetry analysis: the stability of *Pfu*OGT was 80 °C in terms of temperature melting (T_m), if
424 compared with that of *Ss*OGT (68 °C) [89]. It is worth noting that, to obtain the sigmoidal curve for
425 *Pfu*OGT to fit with the Boltzmann equation and calculate the T_m value, a setting of 10 min/°C × cycle
426 have been necessary, whereas the procedure is usually performed at 1 min/°C × cycle [93].

427 *Thermotoga neapolitana* is a hyperthermophilic gram-negative bacterium of the order of
428 Thermotogales [94-96], which are excellent models for genetic engineering and biotechnological
429 applications [97-100]. *T. neapolitana* possesses a CTN1690 ORF showing a clear homology of the
430 O⁶-alkylguanine-DNA-alkyl-transferase. SDS-PAGE *gel-imaging* analysis on lyophilized *T.*
431 *neapolitana* cells incubated with the AGT fluorescent substrate showed a strong fluorescent signal
432 with a molecular weight close to that of *Ss*OGT. The observed molecular weight and, above all, the
433 sensitivity to this O⁶-BG derivative, led to the cloning and heterologous expression of this protein in
434 *E. coli*, then called *Tn*OGT. [89]. This protein, like most AGTs, has a role in DNA repair and was
435 verified with the competitive fluorescent assay in the presence of methylated dsDNA, as described
436 in Figure 3, leading to a IC₅₀ value similar to that obtained with *Ss*OGT. Surprisingly, the enzyme
437 from *T. neapolitana* exhibited a very high activity at low temperatures [89], similar to that shown by
438 the mutant *Ss*OGT-H⁵ (Table 3) [52, 58]. This characteristic hindered the determination of the
439 second order constants at temperatures above 50.0 °C, since its reaction rate went faster than the
440 technical limits of the assay [89]. Superimposition analysis between a *Tn*OGT 3D model and the free
441 form of *Ss*OGT (ID PDB: 4ZYE) revealed in both the presence of a serine residue in the *active site*
442 *loop* (S132 in *Ss*OGT, see Figure 2a), which was replaced in *Ss*OGT-H⁵ by a glutamic acid to
443 improve its activity at lower temperatures. From the superimposition, again, some residues are
444 missing in *Tn*OGT, which play an important role in stabilizing *Ss*OGT. In particular, the ionic
445 interactions that play a crucial role in the stability of the *Saccharolobus* enzyme at high temperatures,
446 such as the pair R133-D27 [39] and the *K-48 network* [59], are mainly replaced by hydrophobic
447 residues in the *Thermotoga* homolog. Evidently, different residues and mechanisms of stabilization
448 contribute to its exceptional catalytic activity at moderate temperatures and the stability at higher
449 ones.

450 5. Future perspectives

451 The interest shown for this class of small proteins for decades has led to useful knowledge
452 from basic research to biotechnological applications [101]. Studies on thermophilic AGTs represent
453 a unique opportunity for structural analysis and, in the case of the *S. solfataricus* protein, for the
454 identification of conformational changes after the trans-alkylation reaction, however not possible
455 with mesophilic AGTs, which in the alkylated form are enormously destabilized [6]. These results
456 could have a wide impact especially in medical fields for the design of novel hMGMT inhibitors to
457 be used in cancer therapy [102]. Furthermore, given their small size, thermophilic enzymes are very
458 useful for studying general stabilization mechanisms at high temperatures (as for *Pk*-MGMT and
459 *Ss*OGT), which can then be applied to mesophilic enzymes. Searching for alternative *Ss*OGT
460 homologues was clearly useful, leading to the identification of AGTs more resistant to thermal

461 denaturation (*Pfu*OGT) or of enzymes with a higher reaction rate at all tested temperatures
462 (*Tn*OGT).

463 Concerning biotechnology, the modification of AGT in a *protein-tag* is an approach to be
464 considered of general applicability, both following a *rational approach*, by abolishing the DNA
465 binding, as in *Ss*OGT-H⁵, and *irrational*, by random mutagenesis and selection of variants for higher
466 catalytic activity, such as SNAP-*tag*[®] [103], or those modified in substrate specificity, such as
467 CLIP-*tag*[®], which is active on benzyl-cytosine (*O*²-BC) derivatives [65]. This knowledge could be the
468 starting point to develop new engineered *thermo*-SNAP-*tag*[®] to be employed in particular
469 biotechnological fields, from *in vivo* studies in (hyper)thermophilic microorganisms (such as the *in*
470 *vivo* CRISPR-Cas immune system in *P. furiosus* [104, 105]) to industrial processes that require high
471 temperatures or, in general, harsh reaction conditions.

472 **Author Contributions:** [§]R.Ma. and R.Me. equally contributed to the present review article.

473 **Funding:** This research was funded by MIUR National Operational Program (PON) Research and Innovation
474 2014-2020 (CCI 2014IT16M2OP005), European Social Fund, Action I.1 "Innovative Doctorates with Industrial
475 characterization".

476 **Acknowledgments:** G.P. would like to thank all the authors, Miss Elena and Elisa Perugino, for their efforts in
477 writing this work, technical assistance, but mainly for human support during the difficult and delicate period
478 of stay-at-home following the COVID-19 outbreak.

479 **Conflicts of Interest:** The authors declare no conflict of interest.

480 Abbreviations

AGT	<i>O</i> ⁶ -alkyl-guanine-DNA-alkyl-transferase
CLIP- <i>tag</i> [®]	engineered version of SNAP- <i>tag</i> [®] active on <i>O</i> ² -BC
FP	auto-fluorescent protein
hMGMT	human <i>O</i> ⁶ -methyl-guanine-DNA-alkyl-transferase
MGMT	<i>O</i> ⁶ -methyl-guanine-DNA-alkyl-transferase
<i>O</i> ² -BC	<i>O</i> ² -benzyl-cytosine
<i>O</i> ⁶ -AG	<i>O</i> ⁶ -alkyl-guanine
<i>O</i> ⁶ -BG	<i>O</i> ⁶ -benzyl-guanine
<i>O</i> ⁶ -MG	<i>O</i> ⁶ -methyl-guanine
OGT	<i>O</i> ⁶ -alkyl-guanine-DNA-alkyl-transferase
SNAP- <i>tag</i> [®]	engineered version of hMGMT for biotech purposes

481 References

- 482 1. Liu, L.; Gerson, S.L. Targeted modulation of MGMT: clinical implications. *Clin. Cancer Res.* **2006**, *12*, 328–
483 331.
- 484 2. Leonard, G.A.; Thomson, J.; Watson, W.P.; Brown T. High-resolution structure of a mutagenic lesion in
485 DNA. *Proc. Natl. Acad. Sci.* **1990**, *87*, 9573–9576.
- 486 3. Drabløs, F.; Feyzi, E.; Aas, P.A.; Vaagbø, C.B.; Kavli, B.; Bratlie, M.S.; Peña-Diaz, J.; Otterlei, M.;
487 Slupphaug, G.; Krokan, H.E. Alkylation damage in DNA and RNA-repair mechanisms and medical
488 significance. *DNA Repair* **2004**, *11*, 1389–1407.
- 489 4. Pegg, A.E. Multifaceted roles of alkyltransferase and related proteins in DNA repair, DNA damage,
490 resistance to chemotherapy, and research tools. *Chem. Res. Toxicol.* **2011**, *24*, 618–639.
- 491 5. Duguid, E.M.; Rice, P.A.; He, C. The structure of the human AGT protein bound to DNA and its
492 implications for damage detection. *J. Mol. Biol.* **2005**, *350*, 657–666.
- 493 6. Daniels, D.S.; Mol, C.D.; Arvai, A.S.; Kanugula, S.; Pegg, A.E.; Tainer, J.A. Active and alkylated human
494 AGT structures: A novel zinc site, inhibitor and extrahelical base binding. *EMBO J.* **2000**, *19*, 1719–1730.
- 495 7. Daniels, D.S.; Woo, T.T.; Luu, K.X.; Noll, D.M.; Clarke, N.D.; Pegg, A.E.; Tainer, J.A. DNA binding and
496 nucleotide flipping by the human DNA repair protein AGT. *Nat. Struct. Mol. Biol.* **2004**, *11*, 714–720.

- 497 8. Tubbs, J.L.; Pegg, A.E.; Tainer, J.A. DNA binding, nucleotide flipping, and the helix-turn-helix motif in
498 base repair by O⁶-alkylguanine-DNA-alkyltransferase and its implications for cancer chemotherapy.
499 DNA Repair **2007**, *6*, 1100–1115.
- 500 9. Xu-Welliver, M.; Pegg, A.E. Degradation of the alkylated form of the DNA repair protein, O⁶-
501 alkylguanine-DNA alkyltransferase. Carcinogenesis **2002**, *23*, 823–830.
- 502 10. Gerson, S.L. MGMT: its role in cancer aetiology and cancer therapeutics. Nat. Rev. Cancer. **2004**, *4*, 296–
503 307.
- 504 11. Sabharwal, A.; Middleton, M.R. Exploiting the role of O⁶-methylguanine-DNA-methyltransferase
505 (MGMT) in cancer therapy. Curr. Opin. Pharmacol. **2006**, *6*, 355–363.
- 506 12. Zhong, Y.; Huang, Y.; Huang, Y.; Zhang, T.; Ma, C.; Zhang, S.; Fan, W.; Chen, H.; Qian, J.; Lu, D. Effects
507 of O⁶-methylguanine-DNA methyltransferase (MGMT) polymorphisms on cancer: a meta-analysis.
508 Mutagenesis **2010**, *25*, 83–95.
- 509 13. Kaina, B.; Christmann, M. DNA repair in personalized brain cancer therapy with temozolomide and
510 nitrosoureas. DNA Repair **2019**, *78*, 128–141.
- 511 14. Khan, O.; Middleton, M.R. The therapeutic potential of O⁶-alkylguanine DNA alkyltransferase inhibitors.
512 Expert Opin. Investig. Drugs **2007**, *10*, 1573–1584.
- 513 15. Paranjpe, A.; Zhang, R.; Ali-Osman, F.; Bobustuc, G.C.; Srivenugopal, K.S. Disulfiram is a direct and
514 potent inhibitor of human O⁶-methylguanine-DNA methyltransferase (MGMT) in brain tumor cells and
515 mouse brain and markedly increases the alkylating DNA damage. Carcinogenesis **2014**, *35*, 692–702.
- 516 16. Rabik, C.A.; Dolan, M.E. Molecular mechanisms of resistance and toxicity associated with platinating
517 agents. Cancer Treat. Rev. **2007**, *33*, 9–23.
- 518 17. Kaina, B.; Margison, G.P.; Christmann, M. Targeting O⁶-methylguanine-DNA methyltransferase with
519 specific inhibitors as a strategy in cancer therapy. Cell Mol. Life Sci. **2010**, *67*, 3663–3681.
- 520 18. Chalfie, M.; Tu, Y.; Euskirchen, G.; Ward, W.W.; Prasher, D.C. Green fluorescent protein as a marker for
521 gene expression. Science **1994**, *263*, 802–805.
- 522 19. Tsien, R.Y. The green fluorescent protein. Annu. Rev. Biochem. **1998**, *67*, 509–554.
- 523 20. di Guan, C.; Li, P.; Riggs, P.D.; Inouye, H. Vectors that facilitate the expression and purification of foreign
524 peptides in *Escherichia coli* by fusion to maltose-binding protein. Gene **1988**, *67*, 1, 21–30.
- 525 21. Schmidt, T.G.M.; Koepke, J.; Frank, R.; Skerra, A. Molecular Interaction Between the Strep-tag Affinity
526 Peptide and its Cognate Target, Streptavidin. J. Mol. Biol. **1996**, *255*, 753–66.
- 527 22. Ren, L.; Chang, E.; Makky, K.; Haas, A.L.; Kaboord, B.; Walid Qoronfle, M. Glutathione S-transferase
528 pull-down assays using dehydrated immobilized glutathione resin. Analytical Biochemistry **2003**, *322*,
529 164–169.
- 530 23. LaVallie, E.R.; DiBlasio, E.A.; Kovacic, S.; Grant, K.L.; Schendel, P.F.; McCoy, J.M. (1993) A thioredoxin
531 gene fusion expression system that circumvents inclusion body formation in the *E. coli* cytoplasm.
532 Bio/Technology **1993**, *11*, 187–193.
- 533 24. Juillerat, A.; Gronemeyer, T.; Keppler, A.; Gendreizig, S.; Pick, H.; Vogel, H.; Johnsson, K. Directed
534 evolution of O⁶-alkylguanine-DNA alkyltransferase for efficient labeling of fusion proteins with small
535 molecules *in vivo*. Chem. Biol. **2003**, *10*, 313–317.
- 536 25. Keppler, A.; Gendreizig, S.; Gronemeyer, T.; Pick, H.; Vogel, H.; Johnsson, K. A general method for the
537 covalent labeling of fusion proteins with small molecules *in vivo*. Nat. Biotechnol. **2003**, *21*, 86–89.
- 538 26. Kindermann, M.; George, N.; Johnsson, N.; Johnsson, K. Covalent and selective immobilization of fusion
539 proteins. J. Am. Chem. Soc. **2003**, *125*, 7810–7811.
- 540 27. Gronemeyer, T.; Chidley, C.; Juillerat, A.; Heinis, C.; Johnsson, K. Directed evolution of
541 O⁶-alkylguanine-DNA alkyltransferase for applications in protein labeling. Protein Eng. Des. Sel. **2006**, *19*,
542 309–316.
- 543 28. Hinner, M.J.; Johnsson, K. How to obtain labeled proteins and what to do with them. Curr. Opin.
544 Biotechnol. **2010**, *21*, 766–776.
- 545 29. Huber, W.; Perspicace, S.; Kohler, J.; Müller, F.; Schlatter, D. SPR-based interaction studies with small
546 molecular weight ligands using hAGT fusion proteins. Anal. Biochem. **2004**, *333*, 280–288.
- 547 30. Niesen, J.; Sack, M.; Seidel, M.; Fendel, R.; Barth, S.; Fischer, R.; Stein, C. SNAP-tag technology: a useful
548 tool to determine affinity constants and other functional parameters of novel anti-body fragments.
549 Bioconjug. Chem. **2016**, *27*, 1931–1941.

- 550 31. Valenti, A.; Napoli, A.; Ferrara, M.C.; Nadal, M.; Rossi, M.; Ciaramella, M. Selective degradation of
551 reverse gyrase and DNA fragmentation induced by alkylating agent in the archaeon *Sulfolobus*
552 *solfataricus*. *Nucleic Acids Res.* **2006**, *34*, 2098–2108.
- 553 32. Kanugula, S.; Pegg, A.E. Alkylation damage repair protein *O*⁶-alkyl-guanine-DNA alkyltransferase from
554 the hyperthermophiles *Aquifex aeolicus* and *Archaeoglobus fulgidus*. *Biochem. J.* **2003**, *375*, 449–455.
- 555 33. Leclere, M.M.; Nishioka, M.; Yuasa, T.; Fujiwara, S.; Takagi, M.; Imanaka, T. The *O*⁶-methylguanine-DNA
556 methyltransferase from the hyperthermophilic archaeon *Pyrococcus* sp. KOD1: a thermostable repair
557 enzyme. *Mol Gen Genet.* **1998**, *258*, 69–77.
- 558 34. Skorvaga, M.; Raven, N.D.; Margison, G.P. Thermostable archaeal *O*⁶-alkylguanine-DNA
559 alkyltransferases. *Proc. Natl. Acad. Sci.* **1998**, *95*, 6711–6715.
- 560 35. Fang, Q.; Kanugula, S.; Pegg, A.E. Function of domains of human *O*⁶-alkyl-guanine-DNA
561 alkyltransferase. *Biochemistry* **2005**, *44*, 15396–15405.
- 562 36. Kanugula, S.; Pegg, A.E. Novel DNA Repair Alkyltransferase from *Caenorhabditis elegans*. *Env. Mol. Mut.*
563 **2001**, *38*, 235–243.
- 564 37. Serpe, M.; Forenza, C.; Adamo, A.; Russo, N.; Perugino, G.; Ciaramella, M.; Valenti, A. The DNA
565 alkylguanine DNA alkyltransferase-2 (AGT-2) of *Caenorhabditis elegans* is involved in meiosis and early
566 development under physiological conditions. *Sci. Rep.* **2019**, *9*, 6889.
- 567 38. Miggiano, R.; Casazza, V.; Garavaglia, S.; Ciaramella, M.; Perugino, G.; Rizzi, M.; Rossi, F. Biochemical
568 and structural studies of the *Mycobacterium tuberculosis* *O*⁶-methylguanine methyltransferase and mutated
569 variants. *J. Bacteriol.* **2013**, *195*, 2728–2736.
- 570 39. Perugino, G.; Miggiano, R.; Serpe, M.; Vettone, A.; Valenti, A.; Lahiri, S.; Rossi, F.; Rossi, M.; Rizzi, M.;
571 Ciaramella, M. Structure-function relationships governing activity and stability of a DNA alkylation
572 damage repair thermostable protein. *Nuc. Ac. Res.* **2015**, *43*, 8801–8816.
- 573 40. Donini, S.; Ferraris, D.M.; Miggiano, R.; Massarotti, A.; Rizzi, M. Structural investigations on orotate
574 phosphoribosyltransferase from *Mycobacterium tuberculosis*, a key enzyme of the *de novo* pyrimidine
575 biosynthesis. *Sci. Rep.* **2017**, *7*, 1180.
- 576 41. Donini, S.; Garavaglia, S.; Ferraris, D.M.; Miggiano, R.; Mori, S.; Shibayama, K.; Rizzi, M. Biochemical and
577 structural investigations on phosphoribosylpyrophosphate synthetase from *Mycobacterium smegmatis*.
578 *PLoS One* **2017**, *12*, 4, e0175815.
- 579 42. Lahiri, S.; Rizzi, M.; Rossi, F.; Miggiano, R.; *Mycobacterium tuberculosis* UvrB forms dimers in solution and
580 interacts with UvrA in the absence of ligands. *Proteins* **2018**, *86*, 98–109.
- 581 43. Presta, L.G.; Rose, G.D. Helix signals in proteins. *Science* **1988**, *240*, 1632–1641.
- 582 44. Richardson, J.S.; Richardson D.C. Amino acid preferences for specific locations at the ends of α -helices.
583 *Science* **1988**, *240*, 1648–1652.
- 584 45. Koscielska-Kasprzak, K.; Cierpicki, T.; Otlewski, J. Importance of alpha-helix N-capping motif in
585 stabilization of betabetaalpha fold. *Protein Sci.* **2003**, *12*, 1283–1289.
- 586 46. Chan, M.K.; Mukund, S.; Kletzin, A.; Adams, M.W.W.; Rees, D.C. Structure of a hyperthermo-philic
587 tungstopterin enzyme, aldehyde ferredoxin oxidoreductase. *Science* **1995**, *267*, 1463–1469.
- 588 47. Miggiano, R.; Perugino, G.; Ciaramella, M.; Serpe, M.; Rejman, D.; Páv, O.; Pohl, R.; Garavaglia, S.; Lahiri,
589 S.; Rizzi, M. Crystal structure of *Mycobacterium tuberculosis* *O*⁶-methylguanine-DNA methyltransferase
590 protein clusters assembled on to damaged DNA. *Biochem. J.* **2016**, *473*, 123–133.
- 591 48. Rice, D.W.; Yip, K.S.; Stillman, T.J.; Britton, K.L.; Fuertes, A.; Connerton, J.; Pasquo, A.; Scandura, R.;
592 Engel, P. C. Insight into the molecular basis of thermal stability from the structure determination of
593 *Pyrococcus furiosus* glutamate dehydrogenase. *FEMS Microbial Rev.* **1996**, *18*, 105–117.
- 594 49. Hashimoto, H.; Inoue, T.; Nishioka, M.; Fujiwara, S.; Takagi, M.; Imanaka, T.; Kai, Y. Hyperthermostable
595 protein structure maintained by intra and inter-helix ion-pairs in archaeal *O*⁶-methylguanine-DNA
596 methyltransferase. *J. Mol. Biol.* **1999**, *292*, 707–716.
- 597 50. Moore, M.H.; Gulbis, J.M.; Dodson, E.J.; Demple, B.; Moody, P.C. Crystal structure of a suicidal DNA
598 repair protein: The Ada *O*⁶-methylguanineDNA methyltransferase from *E. coli*. *EMBO J.* **1994**, *13*, 1495–
599 1501.
- 600 51. Roberts, A.; Pelton, J.G.; Wemmer, D.E. Structural studies of MJ1529, an *O*⁶-methylguanine-DNA
601 methyltransferase. *Magn. Reson. Chem.* **2006**, *44*, S71–S82.

- 602 52. Perugino, G.; Vettone, A.; Illiano, G.; Valenti, A.; Ferrara, M.C.; Rossi, M.; Ciaramella, M. Activity and
603 regulation of archaeal DNA alkyltransferase: Conserved protein involved in repair of DNA alkylation
604 damage. *J. Biol. Chem.* **2012**, *287*, 4222–4231.
- 605 53. Olsson, M.; Lindahl, T. Repair of alkylated DNA in *Escherichia coli*. Methyl group transfer from
606 O⁶-methylguanine to a protein cysteine residue. *J. Biol. Chem.* **1980**, *255*, 10569–10571.
- 607 54. Wu, R.S.; Hurst-Calderone, S.; Kohn, K.W. Measurement of O⁶-alkylguanine-DNA-alkyltransferase
608 activity in human cells and tumor tissues by restriction endonuclease inhibition. *Cancer Res.* **1987**, *47*,
609 6229–6235.
- 610 55. Klein, S.; Oesch, F. Assay for O⁶-alkylguanine-DNA-alkyltransferase using oligonucleotides containing
611 O⁶-methylguanine in a BamHI recognition site as substrate. *Anal. Biochem.* **1992**, *205*, 294–299.
- 612 56. Luu, K.X.; Kanugula, S.; Pegg, A.E.; Pauly, G.T.; Moschel, R.C. Repair of oligodeoxyribonucleotides by
613 O(6)-alkylguanine-DNA alkyltransferase. *Biochemistry* **2002**, *41*, 8689–8697.
- 614 57. Tintoré, M.; Aviñó, A.; Ruiz, F.M.; Eritja, R.; Fábrega, C. Development of a novel fluorescence assay based
615 on the use of the thrombin binding aptamer for the detection of O⁶-alkyl-guanine-DNA alkyltransferase
616 activity. *J. Nuc. Ac.* **2010**, *2010*, 632041.
- 617 58. Vettone, A.; Serpe, M.; Hidalgo, A.; Berenguer, J.; del Monaco, G.; Valenti, A.; Ciaramella, M.; Perugino,
618 G. A novel thermostable protein-tag: optimization of the *Sulfolobus solfataricus* DNA-alkyl-transferase by
619 protein engineering. *Extremophiles* **2016**, *20*, 1–13.
- 620 59. Morrone, C.; Miggiano, R.; Serpe, M.; Massarotti, A.; Valenti, A.; Del Monaco, G.; Rossi, M.; Rossi, F.;
621 Rizzi, M.; Perugino, G. Interdomain interactions rearrangements control the reaction steps of a
622 thermostable DNA alkyltransferase. *Biochim. Biophys. Acta* **2017**, *1861*, 86–96.
- 623 60. Elder, R.H.; Margison, G.P.; Rafferty, J.A. Differential inactivation of mammalian and *Escherichia coli*
624 O⁶-alkylguanine-DNA alkyltransferases by O⁶-benzylguanine. *Biochem. J.* **1994**, *298*, 231–235.
- 625 61. Goodtzova, K.; Kanugula, S.; Edara, S.; Pauly, G.T.; Moschel, R.C.; Pegg, A.E. Repair of O⁶-benzylguanine
626 by the *Escherichia coli* Ada and Ogt and the human O⁶-alkylguanine-DNA alkyltransferase. *J. Biol. Chem.*
627 **1997**, *272*, 8332–8339.
- 628 62. Miggiano, R.; Valenti, A.; Rossi, F.; Rizzi, M.; Perugino, G.; Ciaramella, M. Every OGT Is Illuminated ... by
629 Fluorescent and Synchrotron Lights. *Int. J. Mol. Sci.* **2017**, *18*, 2613–2630.
- 630 63. Melikishvili, M.; Rasimas, J.J.; Pegg, A.E.; Fried, M.G. Interactions of human O(6)-alkylguanine-DNA
631 alkyltransferase (AGT) with short double-stranded DNAs. *Biochemistry* **2008**, *47*, 13754–13763.
- 632 64. Brunk, E.; Mollwitz, B.; Rothlisberger, U. Mechanism to Trigger Unfolding in O⁶-Alkylguanine-DNA
633 Alkyltransferase. *ChemBioChem* **2013**, *14*, 703–710.
- 634 65. Gautier, A.; Juillerat, A.; Heinis, C.; Corrêa, I.R., Jr.; Kindermann, M.; Beaufils, F.; Johnsson, K. An
635 engineered protein-tag for multi-protein labeling in living cells. *Chem. Biol.* **2008**, *15*, 128–136.
- 636 66. Rossi, F.; Morrone, C.; Massarotti, A.; Ferraris, D.M.; Valenti, A.; Perugino, G.; Miggiano, R. Crystal
637 structure of a thermophilic O⁶-alkylguanine-DNA alkyltransferase-derived self-labeling protein-tag in
638 covalent complex with a fluorescent probe. *Biochem. Biophys. Res. Comm.* **2018**, *500*, 698–703.
- 639 67. Cava, F.; de Pedro M.A.; Blas-Galindo, E.; Waldo, G.S.; Westblade, L.F.; Berenguer, J. Expression and use
640 of superfolder green fluorescent protein at high temperatures *in vivo*: a tool to study extreme thermophile
641 biology. *Environ. Microbiol.* **2008**, *10*, 605–613.
- 642 68. Keppler, A.; Pick, H.; Arrivoli, C.; Vogel, H.; Johnsson, K. Labeling of fusion proteins with synthetic
643 fluorophores in live cells. *Proc. Natl. Acad. Sci.* **2004**, *10*, 9955–9959.
- 644 69. Valenti, A.; Perugino, G.; D’Amaro, A.; Cacace, A.; Napoli, A.; Rossi, M.; Ciaramella, M. Dissection of
645 reverse gyrase activities: Insight into the evolution of a thermostable molecular machine. *Nucleic Acids*
646 *Res.* **2008**, *36*, 4587–4597.
- 647 70. Valenti, A.; Perugino, G.; Nohmi, T.; Rossi, M.; Ciaramella, M. Inhibition of translesion DNA polymerase
648 by archaeal reverse gyrase. *Nuc. Ac. Res.* **2009**, *37*, 4287–4295.
- 649 71. Perugino, G.; Valenti, A.; D’Amaro, A.; Rossi, M.; Ciaramella, M. Reverse gyrase and genome stability in
650 hyperthermophilic organisms. *Biochem. Soc. Trans.* **2009**, *37*, 69–73.
- 651 72. Valenti, A.; Perugino, G.; Rossi, M.; Ciaramella, M. Positive supercoiling in thermophiles and mesophiles:
652 of the good and evil. *Biochem. Soc. Trans.* **2011**, *39*, 58–63.
- 653 73. Visone, V.; Han, W.; Perugino, G.; Del Monaco, G.; She, Q.; Rossi, M.; Valenti, A.; Ciaramella, M. *In vivo*
654 and *in vitro* protein imaging in thermophilic archaea by exploiting a novel protein tag. *PLoS ONE* **2017**,
655 *10*, e0185791.

- 656 74. Morita, R.; Nakagawa, N.; Kuramitsu, S.; Masui, R. An O⁶-methylguanine-DNA methyltransferase-like
657 protein from *Thermus thermophilus* interacts with a nucleotide excision repair protein. *J. Biochem.* **2008**,
658 *144*, 267–277.
- 659 75. Schärer, O.D. Alkyltransferase-like Proteins: Brokers Dealing with Alkylated DNA Bases. *Mol. Cell* **2012**,
660 *47*, 3–4.
- 661 76. Tubbs, J.L.; Latypov, V.; Kanugula, S.; Butt, A.; Melikishvili, M.; Kraehenbuehl, R.; Fleck, O.; Marriott, A.;
662 Watson, A.J.; Verbeek, B.; McGown, G.; Thorncroft, M.; Santibanez-Koref, M.F.; Millington, C.; Arvai,
663 A.S.; Kroeger, M.D.; Peterson, L.A.; Williams D.M.; Fried, M.G.; Margison, G.P.; Pegg, A.E.; Tainer, J.A.
664 Flipping of alkylated DNA damage bridges base and nucleotide excision repair. *Nature* **2009**, *459*, 808–
665 813.
- 666 77. Latypov, V.F.; Tubbs, J.L.; Watson, A.J.; Marriott, A.S.; McGown, G.; Thorncroft, M.; Wilkinson, O.J.;
667 Senthong, P.; Butt, A.; Arvai, A.S.; Millington, C.L.; Povey, A.C.; Williams, D.M.; Santibanez-Koref, M.F.;
668 Tainer, J.A.; Margison, G.P.; Adams, C.A.; Fried, M.G. Atf1 regulates choice between global genome and
669 transcription-coupled repair of O(6)-alkylguanines. *Mol Cell.* **2012**, *47*, 50–60.
- 670 78. Zhou Z.; Hartmann, M. Progress in enzyme immobilization in ordered mesoporous materials and related
671 applications. *Chem Soc Rev* **2013**, *42*, 3894–3912.
- 672 79. Tosa T.; Mori T.; Fuse N.; Chibata I. Studies on continuous enzyme reactions. I. Screening of carriers for
673 preparation of water-insoluble aminoacylase. *Enzymologia* **1966**, *31*, 214–224.
- 674 80. Mohamad, N.R.; Che Marzuki, N.H.; Buang, N.A.; Huyop, F.; Wahab, R.A. An overview of technologies
675 for immobilization of enzymes and surface analysis techniques for immobilized enzymes. *Biotech.*
676 *Biotech. Equip.* **2015**, *29*, 205–220.
- 677 81. Nguyen, H.H.; Kima, M. An Overview of Techniques in Enzyme Immobilization. *App. Sci. Conv. Tech.*
678 **2017**, *26*, 157–163.
- 679 82. Jakub Zdarta, J.; Meyer, A.S.; Jesionowski, T.; Pinelo, M. A General Overview of Support Materials for
680 Enzyme Immobilization: Characteristics, Properties, Practical Utility. *Catalysts* **2018**, *8*, 92.
- 681 83. Sirisha, V.L.; Jain, A.; Jain, A. Chapter Nine - Enzyme Immobilization: An Overview on Methods, Support
682 Material, and Applications of Immobilized Enzymes. *Adv. Food Nut. Res.* **2016**, *79*, 179–211.
- 683 84. Gurian-Sherman, D.; Lindow, S.E. Bacterial ice nucleation: significance and molecular basis. *FASEB J.*
684 **1993**, *7*, 1338–1343.
- 685 85. Cochet, N.; Widehem, P. Ice crystallization by *Pseudomonas syringae*. *Appl. Microbiol. Biotechnol.* **2000**, *54*,
686 153–161.
- 687 86. Merlo, R.; Del Prete, S.; Valenti, A.; Mattosovich, R.; Carginale, V.; Supuran, C.T.; Capasso, C.; Perugino,
688 P. An AGT-based protein-tag system for the labelling and surface immobilization of enzymes on *E. coli*
689 outer membrane. *J. Enz. Inhib. Med. Chem.* **2019**, *34*, 490–499.
- 690 87. Del Prete, S.; Merlo, R.; Valenti, A.; Mattosovich, R.; Rossi, M.; Carginale, M.; Supuran, C.T.; Perugino,
691 G.; Capasso, C. Thermostability enhancement of the α -carbonic anhydrase from *Sulfurihydrogenibium*
692 *yellowstonense* by using the anchoring-and-selflabelling-protein-tag system (ASL^{tag}). *J. Enz. Inhib. Med.*
693 *Chem.* **2019**, *34*, 946–954.
- 694 88. Del Prete, S.; Perfetto, R.; Rossi, M.; Alasmay, F.A.S.; Osman, S.M.; AlOthman, Z.; Supuran, C.T.;
695 Capasso, C. A one-step procedure for immobilising the thermostable carbonic anhydrase (SspCA) on the
696 surface membrane of *Escherichia coli*. *J. Enz. Inhib. Med. Chem.* **2017**, *32*, 1120–1128.
- 697 89. Mattosovich, R.; Merlo R.; Fontana, A.; d'Ippolito, G.; Terns, M.P; Watts, E.A.; Valenti, A.; Perugino, P. A
698 journey down to hell: new thermostable protein-tags for biotechnology at high temperatures.
699 *Extremophiles* **2020**, *24*, 81–91.
- 700 90. Fiala, G.; Stetter, K.O. *Pyrococcus furiosus* sp. nov. represents a novel genus of marine heterotrophic
701 archaeobacteria growing optimally at 100 °C. *Arch. Microb.* **1986**, *145*, 56–61.
- 702 91. Lundberg, K.S.; Shoemaker, D.D.; Adams, M.W.W.; Short, J.M.; Sorge, J.A.; Mathur, E.J. High-fidelity
703 amplification using a thermostable DNA polymerase isolated from *Pyrococcus furiosus*. *Gene* **1991**, *108*, 1–
704 6.
- 705 92. Nishikori, S.; Shiraki, K.; Yokota, K.; Izumikawa, N.; Fujiwara, S.; Hashimoto, H.; Imanaka, T.; Takagi, M.
706 Mutational effects on O⁶-methylguanine-DNA methyltransferase from hyperthermophile: contribution of
707 ion-pair network to protein thermostability. *J. Biochem.* **2004**, *135*, 525–532.
- 708 93. Niesen F.H.; Berglund, H.; Vedadi, M. The use of differential scanning fluorimetry to detect ligand
709 interactions that promote protein stability. *Nat Protoc* **2007**, *2*, 2212–2221.

- 710 94. Belkin, S.; Wirsén, C.O.; Jannasch, H.W. A new sulfur-reducing, extremely thermophilic eubacterium
711 from a submarine thermal vent. *App. Environ. Microbiol.* **1986**, *51*, 1180–1185.
- 712 95. Jannasch, H.W.; Huber, R.; Belkin, S.; Stetter, K.O. *Thermotoga neapolitana* sp. nov. of the extremely
713 thermophilic, eubacterial genus *Thermotoga*. *Arch. Microbiol.* **1988**, *150*, 103–104.
- 714 96. Connors, S.B.; Mongodin, E.F.; Johnson, M.R.; Montero, C.I.; Nelson, K.E.; Kelly, R.M. Microbial
715 biochemistry, physiology, and biotechnology of hyperthermophilic *Thermotoga* species. *FEMS Microb.*
716 *Rev.* **2006**, *30*, 872–905.
- 717 97. Zhang, J.; Shi, H.; Xu, L.; Zhu, X.; Li, X. Site-directed mutagenesis of a hyperthermophilic endoglucanase
718 Cel12B from *Thermotoga maritima* based on rational design. *PLoS ONE* **2015**. doi. org/10.1371/journ
719 al.pone.0133824
- 720 98. Fink, M.; Trunk, S.; Hall, M.; Schwab, H.; Steiner, K. Engineering of TM1459 from *Thermotoga maritima* for
721 increased oxidative alkene cleavage activity. *Front. Microb.* **2016**, *7*, 1–9.
- 722 99. Donaldson, T.; Iozzino, L.; Deacon, L.J.; Billones, H.; Ausili, A.; D’Auria, S.; Dattelbaum, J.D. Engineering
723 a switch-based biosensor for arginine using a *Thermotoga maritima* periplasmic binding protein. *An.*
724 *Biochem.* **2017**, *525*, 60–66.
- 725 100. Han, D.; Xu, Z. Development of a pyrE-based selective system for *Thermotoga* sp. strain RQ7.
726 *Extremophiles* **2017**, *21*, 297–306.
- 727 101. Pegg, A.E. Repair of *O*⁶-alkylguanine by alkyltransferases. *Mutat. Res.* **2000**, *462*, 83–100.
- 728 102. Margison, G.P.; Povey, A.C.; Kaina, B.; Santibanez Koref, M.F. Variability and regulation of
729 *O*⁶-alkylguanine-DNA alkyltransferase. *Carcinogenesis* **2003**, *24*, 625–635.
- 730 103. Mollwitz, B.; Brunk, E.; Schmitt, S.; Pojer, F.; Bannwarth, M.; Schiltz, M.; Rothlisberger, U.; Johnsson, K.
731 Directed evolution of the suicide protein *O*⁶-alkylguanine-DNA alkyltransferase for increased reactivity
732 results in an alkylated protein with exceptional stability. *Biochemistry* **2012**, *51*, 986–994.
- 733 104. Hale, C.R.; Zhao, P.; Olson, S.; Duff, M.O.; Graveley, B.R.; Wells, L.; Terns, R.M.; Terns, M.P. RNA-guided
734 RNA cleavage by a CRISPR RNA-Cas protein complex. *Cell* **2009**, *139*, 945–956.
- 735 105. Terns, R.M.; Terns, M.P. The RNA- and DNA-targeting CRISPR-Cas immune systems of *Pyrococcus*
736 *furiosus*. *Biochem. Soc. Trans.* **2013**, *41*, 1416–1421.
- 737
738



© 2020 by the authors. Submitted for possible open access publication under the terms and conditions of the Creative Commons Attribution (CC BY) license (<http://creativecommons.org/licenses/by/4.0/>).